nisms discussed in this report are sufficient to account for many long-term population cycles of forest insects.

Systematic acquisition of more data will allow these ideas to be subjected to additional tests similar to that of Fig. 2. The model represented by Eqs. 3, 5, and 6 is of more than academic interest as it enables us to calculate the rate at which a virus or other pathogen must be artificially introduced if it is to be effective in the control, or extinction, of a population of insect pests (*14*). Beyond this, evolutionary aspects of the association between invertebrate hosts and their pathogens (*1*, *27*) must be examined; we have focused only on the dynamics of existing associations.

ROY M. ANDERSON
Zoology Department, Imperial College, London University, Prince Consort Road, London, SW7, England
ROBERT M. MAY
Biology Department, Princeton University, Princeton, New Jersey, 08544

References and Notes

1. P. W. Price, *Evolutionary Biology of Parasites* (Princeton Univ. Press, Princeton, N.J., 1980); H. D. Crofton, *Parasitology* **63**, 179 and 343 (1971); R. M. Anderson and R. M. May, *J. Anim. Ecol.* **47**, 219 (1978); K. R. Barbehenn, *Biotropica* **1**, 29 (1969); H. Cornell, *Am. Nat.* **108**, 880 (1974); C. A. Lanciani, *Ecology* **56**, 689 (1975); G. R. Stairs, *Annu. Rev. Entomol.* **17**, 355 (1972).
2. R. M. Anderson and R. M. May, *Nature (London)* **280**, 361 and 455 (1979).
3. N. T. J. Bailey, *The Mathematical Theory of Infectious Diseases* (Griffin, London, 1975).
4. K. Dietz, in *Epidemiology*, D. Ludwig and K. L. Cooke, Eds. (S.I.A.M. Publications, Philadelphia, 1975), pp. 104–121.
5. See, for example, C. J. Krebs, *Ecology* (Harper & Row, New York, 1972); M. P. Hassell, *Dynamics of Arthropod Prey-Predator Systems* (Princeton Univ. Press., Princeton, N.J., 1978).
6. C. J. Bayne, *Malacol. Rev.* **6**, 13 (1973); F. B. Bang, *BioScience* **23**, 584 (1973); K. Maramorosch and R. E. Shope, Eds., *Invertebrate Immunity* (Academic Press, New York, 1975).
7. In many cases, the parasite's life cycle involves one or more intermediate host species (for example, the mosquitoes that malarial *Plasmodium* species use as a developmental stage on the way from one human host to the next, or the snail vectors involved in the transmission of schistosomiasis). A brief review of the complications thus introduced by indirect transmission from one primary host to the next is in (*2*).
8. The proportionality coefficient β in this transmission term is the hardest parameter to measure in practical applications. If the age-specific prevalence of the infection in the host population is known, and is in equilibrium, β can sometimes be estimated indirectly from the typical age at which the infection is acquired (*4*).
9. This notion of the infection's "basic reproductive rate" is discussed more fully by J. A. Yorke, N. Nathanson, G. Pianigiani, and J. Martin [*Am. J. Epidemiol.* **109**, 103 (1978)] and R. M. Anderson [in *The Mathematical Theory of the Dynamics of Populations*, R. W. Hiorns, Ed. (Blackwell, Oxford, in press)].
10. W. O. Kermack, and A. G. McKendrick, *Proc. R. Soc. London Ser. A* **115**, 700 (1927).
11. In this case, the equilibrium value of the host population is $N^* = N_T/(1 - r/\alpha)$, with $r = a - b$ and $N_T = (\alpha + b + \gamma)/\beta$ as discussed in the text. Of this population, a fraction r/α is infected.
12. If $\alpha < r$ (with $r = a - b$), the host population grows at the diminished rate $r - \alpha$ for $N >> N_T$. We have elsewhere (*2*) argued that trends in human population growth over the past 10,000 years or so exemplify this general pattern.
13. M. P. Hassell, J. H. Lawton, R. M. May, *J. Anim. Ecol.* **45**, 471 (1976).
14. R. M. Anderson and R. M. May, *Philos. Trans. R. Soc. London Ser. B*, in press.
15. In particular, long-term experiments on laboratory mice infected with the bacterium *Pasteurella muris* and with the mousepox virus ectromelia have been analyzed in this way (*2*). See also R. M. May and R. M. Anderson [*J. Anim. Ecol.* **47**, 249 (1978)].
16. R. P. Jacques, *Misc. Publ. Entomol. Soc. Am.* **10**, 99 (1977).
17. K. M. Smith, *Virus-Insect Relationships* (Longman, London, 1976).
18. For further discussion, see T. W. Tinsley [*Annu. Rev. Entomol.* **24**, 63 (1979)] and P. F. Entwistle, P. H. W. Adams, H. F. Evans [*J. Invertebr. Pathol.* **30**, 15 (1977)].
19. An infected host that releases Λ infective particles into the environment when it dies is essentially equivalent to a host that produces infective stages at a steady rate $\lambda = \Lambda\ (\alpha + b + \gamma)$ throughout the expected lifetime, $1/(\alpha + b + \gamma)$, of its infection.
20. Specifically, we require $\lambda > A$, where $A = \alpha(\alpha + b + \gamma)/(\alpha - r)$. As documented in (*14*), actual values of λ are typically very large.
21. For $\lambda > A$ [A defined as in (*20*)] and $\alpha > r$ ($r = a - b$), Eqs. 3, 5, and 6 give a nontrivial solution corresponding to a locally stable point if
$$[\mu + (A - r)(1 - A/\lambda)][A - \alpha] - [1 - A/\lambda]^2\alpha(\alpha + b + \gamma) > 0$$
Conversely, if this expression is negative, there is a stable limit cycle. In the limit $\lambda >> A$, which is true in most real situations (*14*), this criterion reduces to
$$(\mu + A - r)(A - \alpha) - \alpha(\alpha + b + \gamma) > 0$$
It is clear that cycles are most likely to arise when α is large and μ is small. Notice that these dynamical criteria do not involve the transmission coefficient ν, which enters only in the scaling of the variables N, Y, and W.
22. The data are from C. Auer [*Z. Angew. Entomol.* **62**, 202 (1968)].
23. W. Baltensweiler [*Can. Entomol.* **96**, 792 (1964)] has surveyed data showing the larch bud moth in the Engadine Valley has exhibited 9- to 10-year cycles for more than 100 years. See also A. Fischlin and W. Baltensweiler, *Bull. Soc. Entomol. Suisse* **52**, 273 (1979).
24. As discussed more fully in (*14*), we use the information in W. Baltensweiler, G. Benz, P. Borey, and V. Delucchi [*Annu. Rev. Entomol.* **22**, 79 (1977)], in G. Benz [*Agron. Glas.* **62**, 566 (1962)], and in (*23*, *24*) to assign the parameter values (units in years): $a - b \approx 1$ (a necessarily rough estimate); $b \approx 3.3$ ($1/b$ around 3.5 months); $\gamma \approx 0$; $\alpha \approx 14$; $\lambda \approx 10^6$ (effectively infinite); $\mu \approx 3.0$ ($1/\mu$ around 3 to 4 months). The transmission coefficient ν is set arbitrarily at $\nu = 10^{-10}$.
25. J. A. Yorke and W. P. London, *Am. J. Epidemiol.* **98**, 469 (1973); K. Dietz, in *Mathmatical Models in Medicine*, S. A. Levin, Ed. (Springer-Verlag, New York, 1976), pp. 1–15.
26. R. M. May, Ed., *Theoretical Ecology* (Blackwell, Oxford, 1976), chaps. 2, 4, 5, and 6.
27. F. L. Black *et al.*, *Am. J. Epidemiol.* **100**, 230 (1974); J. H. Gillespie, *Ecology* **56**, 49.3 (1975); I. Eshel, *Theor. Popul. Biol.* **11**, 410 (1977); S. A. Levin and D. Pimentel, *Am. Nat.*, in press; A. A. Berryman, *Res. Popul. Ecol. (Kyoto)* **19**, 181 (1978).
28. G. G. Thompson and D. W. Scott, *J. Invertebr. Pathol.* **33**, 57 (1979).
29. M. L. Prebble and K. Graham, *B.C. Lumberman* **29**, 37 (1945); C. A Miller, *Can. Entomol.* **98**, 592 (1966).
30. H. Klomp, *Adv. Ecol. Res.* **3**, 207 (1966).
31. F. T. Bird and D. E. Elgee, *Can. Entomol.* **139**, 371 (1957).
32. A. C. Hodson, *Tech. Bull. Minn. Agric. Exp. Stn.* **148**, 1 (1941); H. M. Thomson, *Bi-mon. Prog. Rep. Div. For. Biol. Ottawa* **16** (No. 4), 1 (1960).
33. We thank M. P. Hassell, T. R. E. Southwood, and two anonymous reviewers for helpful comments. This work was supported in part by NSF grant DEB79-03290.

2 February 1980; revised 16 July 1980

Reorganization of the Axon Membrane in Demyelinated Peripheral Nerve Fibers: Morphological Evidence

Abstract. *Cytochemical staining of demyelinated peripheral axons revealed two types of axon membrane organization, one of which suggests that the demyelinated axolemma acquires a high density of sodium channels. Ferric ion–ferrocyanide stain was confined to a restricted region of axon membrane at the beginning of a demyelinated segment or was distributed throughout the demyelinated segment of axon. The latter pattern represents one possible morphological correlate of continuous conduction through a demyelinated segment and suggests a reorganization of the axolemma after demyelination.*

At least three responses have been demonstrated when an action potential arrives at a demyelinated segment of an axon. Conduction block may occur if the demyelinated axolemma is inexcitable (*1*, *2*) or as a result of impedance mismatch (*3*, *4*). Slowed saltation of action potentials between nodes of Ranvier results when passive internodal properties are altered due to loss of myelin (5). Finally, continuous conduction can occur across demyelinated internodal membranes that possess electrical excitability (*6*, *7*).

In normal myelinated fibers, Na^+ channels are concentrated at the nodes of Ranvier; in the internodal axolemma their density is lower than that necessary to sustain conduction (*2*). It has been suggested that demyelinated axonal regions develop electrical excitability, much as denervated muscle develops hypersensitivity (*2*). Electrophysiological observations of continuous conduction in demyelinated axons (*6*, *7*) indicate that internodal membranes undergo reorganization resulting in the development of electrical excitability. The physiological observations (*6*, *7*) suggest that (i) Na^+ channels and associated structures remain aggregated in clusters that become distributed along the length of the axon, (ii) reorganization of the axon membrane occurs such that individual Na^+ channels are dispersed through the demyelinated internodal membrane, and/or (iii) new channels are added to the demyelinated axon membrane.

Although the structural heterogeneity (*8*) of the axolemma of normally myeli-

0036-8075/80/1107-0661$00.50/0

nated axons is clearly established (*2*, *9–11*), sufficient anatomical evidence has yet to be presented to illustrate the morphological basis of abnormal modes of conduction in demyelinated fibers or to demonstrate structural modification of the axon membrane. This report provides morphological evidence showing that in some demyelinated fibers the axolemma reorganizes into a configuration that can sustain continuous conduction.

Fibers from the peroneal nerve of adult male Wistar rats, demyelinated by crushing (*12*), were examined. Seven to 30 days after the sciatic nerve was crushed, the peroneal nerve distal to the crushed area was excised, immersed in fixative for 3 hours, and stained by the ferric ion–ferrocyanide (FeFCN) cytochemical technique (*13*). We previously summarized evidence indicating that this staining technique provides a cytochemical marker for regions of high Na^+ channel density (*14*).

Figure 1 shows electron micrographs of demyelinated peroneal nerve fibers 16 days after the sciatic nerve was crushed for 30 seconds with watchmaker's forceps. This interval offers examples of demyelination, remyelination, and regeneration. Figure 1A illustrates the pattern of FeFCN staining in a heminode, one of the common stages of demyelination observed after this survival period. The axon (*a*) is myelinated (*m*, myelin) on one side of the stained area (left of the bracket) and is demyelinated on the other side (right of the bracket). A Schwann cell (*s*) has established a one-to-one relationship with the demyelinated segment, suggesting that remyelination is imminent for that segment (*e*, extracellular space). The region of the axon shown in Fig. 1B (from the bracketed region in Fig. 1A) has accumulated only a moderate amount of FeFCN stain (between arrows) and this is confined to the axoplasmic side of the axolemma for a 1-μm region (the length of a normal node of Ranvier) adjacent to the last terminal loop of the myelinated side. Axoplasm in the region beneath the stained axolemma is more electron-dense than contiguous axoplasm or internodal axoplasm of neighboring axons. This pattern of staining resembles the pattern observed at normal nodes of Ranvier (*2*, *10*, *11*), in that the length of the zone of FeFCN staining in the demyelinated fiber is restricted to ~ 1 μm. No apparent Schwann cell specializations form the right boundary of the stained region.

In contrast, the axon shown in Fig. 1C (a photomontage of electron micrographs of the same tissue as in Fig. 1, A and B) has a demyelinated region 12 μm long and is characterized by dense staining distributed throughout the demyelinated zone on the cytoplasmic surface of the axolemma. This stained demyelinated zone retains two well-defined areas of very dense stain (arrowheads mark the inner boundary) adjacent to degenerating myelin and networks of fingerlike processes (p_1, p_2). Distinct subaxolemmal aggregates of stain (insets in Fig. 1C) are distributed throughout the demyelinated region (*15*). While the FeFCN staining appears to be uneven in the demyelinated zone, its distribution throughout this region is relatively continuous. Adjacent regenerating axons (such as a_1), with or without myelin sheaths in the same section, are not stained beneath the axolemma. However, in this material there were many examples of normally stained nodes with the stain present at the nodal axolemma, as in normal tissue. Examination of serial sections revealed that the axolemma of axon *a* (Fig. 1C) is densely stained in the demyelinated region, in contrast to axolemma wrapped by compact myelin, which is not stained.

The neurophysiological data for demyelinated fibers are consistent with several patterns of distribution of Na^+ channels and associated structures. For example, the channels can be concen-

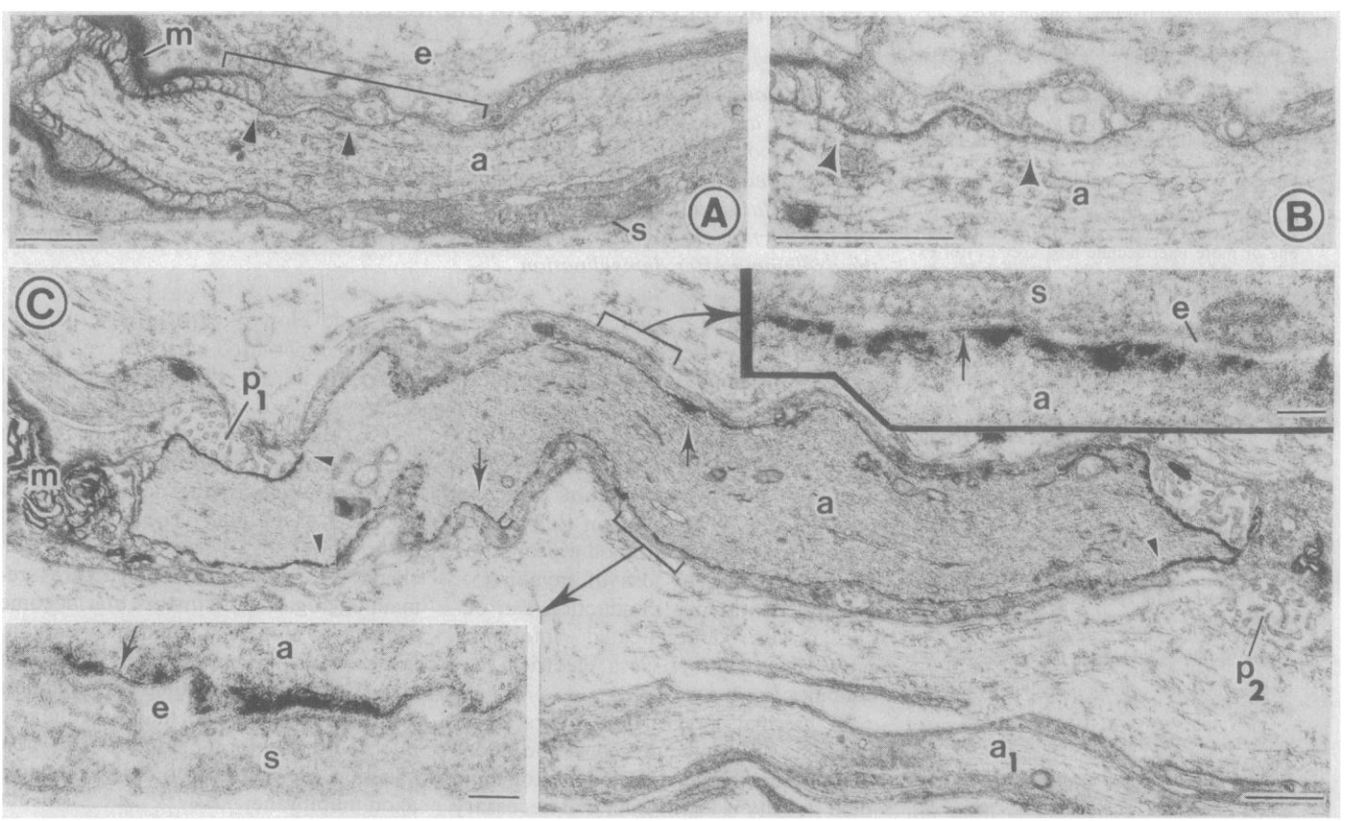

Fig. 1. Electron micrographs of demyelinated nerve fibers stained by the ferric ion–ferrocyanide technique. Scale bars: (A), (B), and (C), 1μM; insets, 0.1 μm.

trated in patches at separate nodal regions so as to allow for distinct zones of inward current, thereby causing slowed saltation (*5*) and conduction block. Alternatively, the distribution of the channels can be relatively continuous, allowing for spatially continuous inward current (*6, 7*) and continuous conduction along the demyelinated region.

Our results suggest morphological correlates for both predicted patterns of organization of the axolemma in peripheral demyelinated axons. Figure 1, A and B, presents the anatomical correlate of the type of axonal membrane that might conduct with slowed saltation or exhibit conduction blocking. When an action potential reaches the demyelinated zone from the myelinated portion of the fiber, conduction may be blocked because of reduced excitability of the demyelinated membrane (*1, 2*) or impedance mismatch at the junction of the myelinated and demyelinated regions (*3, 4*). Saltation may continue, although slowed because of changes in passive properties of the internodal membrane, namely an increase in internodal capacitance and a decrease in internodal transverse resistance (*5*).

The electron micrograph in Fig. 1C presents a possible morphological correlate of continuous conduction. The spatial distribution of FeFCN stain that we have described suggests a high density of Na^+ channels along the demyelinated (former paranodal or internodal) region. This pattern of staining offers one morphological correlate for the physiological observation of spatially continuous inward current associated with continuous conduction along the demyelinated axon. In this case the demyelinated axolemma, which presumably contained a low density (*2*) of Na^+ channels prior to demyelination, reorganized by redistributing channels or by acquiring new ones.

These data concerning reorganization of the axon membrane after demyelination are of interest not only in terms of understanding the pathophysiology of demyelinated fibers, but also with respect to the mechanisms that mediate subsequent recovery of conduction. Future studies incorporating freeze-fracture or pharmacological methods should provide further information about this phenomenon.

ROBERT E. FOSTER
CHRISTOPHER C. WHALEN
STEPHEN G. WAXMAN
Department of Neurology, Stanford University School of Medicine, Veterans Administration Medical Center, Palo Alto, California 94304

References and Notes

1. Z. J. Koles and M. Rasminsky, *J. Physiol. (London)* **227**, 351 (1972).
2. J. M. Ritchie and R. B. Rogart, *Proc. Natl. Acad. Sci. U.S.A.* **74**, 211 (1977).
3. S. G. Waxman, *Neurology* **28**, 27 (1978).
4. T. A. Sears, H. Bostock, M. Sherratt, *ibid.*, p. 21; H. Bostock, R. M. Sherratt, T. A. Sears, *Nature (London)* **274**, 385 (1978).
5. M. Rasminsky and T. A. Sears, *J. Physiol. (London)* **227**, 323 (1972).
6. H. Bostock and T. A. Sears, *Nature (London)* **263**, 786 (1976).
7. ———, *J. Physiol. (London)* **280**, 273 (1978).
8. Using ^3H-labeled saxitoxin, Ritchie and Rogart (*2*) showed that in the normally myelinated axon, Na^+ channels are concentrated in nodal axolemma and are present at a very low density in the internodal axolemma. Likewise, a high density of external-face intramembranous particles (*9*) and a specific pattern of FeFCN staining (*10, 11*) are found at the node, indicating specialization of the nodal membrane.
9. J. Rosenbluth, *J. Neurocytol.* **5**, 731 (1976); C. Kristol, K. Akert, C. Sandri, U. Wyss, M. V. L. Bennett, H. Moor, *Brain Res.* **125**, 197 (1977); C. Kristol, C. Sandri, K. Akert, *ibid.* **142**, 391 (1978).
10. D. C. Quick and S. G. Waxman, *J. Neurol. Sci.* **31**, 1 (1977); S. G. Waxman, W. G. Bradley, E. A. Hartwieg, *Proc. R. Soc. London Ser. B* **201**, 301 (1978).
11. S. G. Waxman and D. C. Quick, *J. Neurol. Neurosurg. Psychiatry* **40**, 379 (1977).
12. D. Denny-Brown and C. Brenner, *Arch. Neurol. Psychiatry* **52**, 1 (1944); J. Ochoa, T. J. Fowler, R. W. Gilliatt, *J. Anat.* **113**, 433 (1972). The results described are not due to crushing per se, since we made similar observations using the JHM model of virus-induced demyelination [R. E. Foster, C. C. Whalen, S. G. Waxman, L. P. Weiner, *J. Cell Biol.* **87**, 68a (1980)].
13. The tissue was fixed for 3 hours in cold 5 percent glutaraldehyde buffered with 0.2*M* sodium cacodylate (*p*H 7.4; 360 mOsm), washed three times in fresh 0.2*M* cacodylate buffer, postfixed for $1^1/_2$ hours in 2 percent OsO_4, washed in distilled water three times at 5 minutes per wash, and stained by the FeFCN technique. For this the tissue sample was placed in 0.01*M* ferric chloride, washed three times in distilled water (5 minutes per wash), placed in 1 percent potassium ferrocyanide, and washed two more times in distilled water. The sample was then dehydrated and embedded in Epon-Araldite (*11*). Thick (3 μm) serial sections were examined by light microscopy, and selected thick sections were reembedded. Ultrathin sections were cut from these, stained on a grid with aqueous uranyl acetate and Reynold's lead citrate, and examined with a JEOL 100 CX electron microscope.
14. In normal mammalian peripheral nerve, the FeFCN technique stains the cytoplasmic surface of the axon membrane at nodes of Ranvier but not at internodal regions of the same fibers. Absence of internodal membrane staining was shown not to be due to lack of ability of the stain to reach these areas (*10, 11*). Specific staining of initial segment membrane rather than soma or dendritic membrane is consistent with the hypothesis that this stain is specific to regions densely supplied with Na^+ channels [S. G. Waxman and D. C. Quick, in *Physiology and Pathobiology of Axons*, S. G. Waxman, Ed. (Raven, New York, 1978), pp. 125–130]. In the electrocyte axons of *Sternarchus albifrons*, in which there are both excitable and inexcitable nodes [M. V. L. Bennett, in *Fish Physiology*, W. S. Hoar and D. J. Randall, Eds. (Academic Press, New York, 1971), pp. 374–491; S. G. Waxman, G. D. Pappas, M. V. L. Bennett, *J. Cell Biol.* **53**, 210 (1972)], the excitable nodes stain densely with FeFCN while inexcitable nodes along the same fiber do not (*10*). It should be emphasized that absence of staining with FeFCN does not necessarily imply membrane inexcitability, since C fibers are not stained with this technique (*11*). Sodium channel density for C fibers, estimated from measurements of the binding of ^3H-labeled saxitoxin, is approximately 110 per square micrometer [J. M. Ritchie, R. B. Rogart, G. R. Strichartz, *J. Physiol. (London)* **261**, 477 (1976)]. Axolemma staining with FeFCN thus appears to reflect quantitative differences in membrane structure.
15. This staining is not due to preferential accessibility of the demyelinated membrane to the extracellular milieu, since C fibers do not stain even when directly exposed to the extracellular space (*11*), and since the inexcitable type II nodes in *S. albifrons* (*14*) also do not stain.
16. Supported in part by NIH grant NS-15320, National Multiple Sclerosis Society grant RG-1231, and by the Medical Research Service of the Veterans Administration. We thank S. Cameron and M. Smith for technical assistance.

13 May 1980; revised 30 June 1980

Aspirin: An Unexpected Side Effect on Prostacyclin Synthesis in Cultured Vascular Smooth Muscle Cells

Abstract. *Monolayer cultures of rat aorta smooth muscle cells synthesized the anti-aggregatory substance prostacyclin via the cyclooxygenase pathway from ^{14}C-labeled arachidonic acid. The product was identified both by bioassay and by mass spectrometry. Labeled cells produced prostacyclin only when exposed to the initiator thrombin: treatment with therapeutic concentrations of aspirin (0.2 millimolar) for 30 minutes completely destroyed the cells' ability to synthesize prostacyclin. Prostacyclin synthesis from exogenous arachidonic acid recovered fully within 1 to 2 hours by a cycloheximide-sensitive process. Thrombin responsiveness, which was permanently impaired in confluent nondividing cultures, recovered substantially and within 24 hours only when cells were stimulated to divide by subculturing. These results indicate that resting vascular cells can rapidly synthesize new cyclooxygenase, but that aspirin destroys additional components of the prostacyclin system which can only be replaced during cell division.*

Thromboxane (TXA_2) and prostacyclin (PGI_2) are synthesized from arachidonic acid by way of a common endoperoxide precursor (*1, 2*). When synthesized in platelets, TXA_2 stimulates aggregation and is a vasoconstrictor (*3*); in contrast, PGI_2 synthesized in blood vessel walls is a potent inhibitor of aggregation and acts as a vasodilator (*4*).

A common property underlying the action of a number of antiplatelet drugs such as aspirin is their ability to inhibit the cyclooxygenase enzyme that converts arachidonic acid to the cyclic endoperoxide intermediate and thus to prevent the synthesis of the proaggregatory substance TXA_2 in platelets (*5*). A number of these drugs are being tested both

0036-8075/80/1107-0663$00.50/0